Joint power optimization and scaled beamforming approach in B5G network based massive MIMO enabled HetNet with full-duplex small cells

Malini Balachandran[1] · Noor Mohammed Vali Mohamad[1]

Abstract

Fifth generation (5G) mobile communication networks have the ability to deal with the growing need for increased data rates, decreased network latencies, low power consumption, seamless coverage, and massive connectivity while sustaining the high Quality of Service (QoS) at the subscriber's end. The key drivers of beyond 5G (B5G) are anticipated to be the convergence of all the features of 5G and B5G becomes more heterogeneous with the different small cell access points and massive multiple-input multiple-output (massive MIMO). In this work, the macro base station enabled with massive MIMO technology and the small cell access points possessing the full-duplex communication ability in a heterogeneous network (HetNet) is investigated. The prime objective is to optimize the power utilization by employing scaled beamforming and power allocation techniques with reduced complexity while sustaining the QoS in a full-duplex massive MIMO enabled HetNet with small cells. The joint power optimization and scaled beamforming algorithm is used to maximize the sum rates with reduced power consumption when compared to multi-flow zero-forcing (MZF) beamforming. The complexity analysis is also carried out by optimizing the number of transmission antennas and users.

1 Introduction

The emergence of new wireless devices and the ever-escalating demand for voice and data traffic indicates the need to evolve and meet the high capacity and coverage requirements of the wireless network. Cisco Visual Networking Index (VNI) estimates a sevenfold growth in the worldwide data traffic from 2017 to 2020 [1]. This necessitates the 5G wireless communication networks to introduce new technologies to address the high data rate, seamless coverage, high capacity demand with low power consumption, and maintaining QoS. The massive MIMO technology and dense heterogeneous networks (HetNet) have been identified as an inevitable solution to address the unprecedented capacity demand

✉ Noor Mohammed Vali Mohamad
noorb4u@gmail.com

[1] School of Electronics Engineering, Vellore Institute of Technology, Vellore, India

with better energy efficiency [2]. Massive MIMO is a technology where the macro base station is furnished with massive antennas to serve the clients concurrently at the same time and frequency resource. These massive antennas make sure to provide better signal energy focus on the anticipated users which results in high spectral efficiency (SE) and energy efficiency (EE) under realistic scenarios [3–5]. Further, the massive MIMO utilizes degrees of freedom and offers services to its clients at the same time and frequency band thus enhancing throughput of the system. The propagation channels corresponding to various users in the massive MIMO network decorrelate when the number of the antenna array is increased [6]. Massive MIMO can smartly utilize the 5G spectrum and it is capable of extending the coverage through high gain beamforming strategy and higher order spatial multiplexing [7]. Massive MIMO operates in time division duplex (TDD) mode to acquire channel state information for the utilization of channel reciprocity [8]. Time division duplex (TDD) mode of operation enables the users to utilize the same time and frequency resource thereby minimizing the feedback overhead and channel training in the downlink [9]. In a dense HetNet with small cell access points (SCAs), are cost-effective low power base stations that can provide capacity and coverage

enhancements ensuring QoS. Along with the typical macro base station, enormous small cell access points (SCAs) are deployed to relieve the traffic from the macro base station. Moreover, it could lead to the problem of routing the traffic that arises from SCAs to the backhaul network. Enabling wired backhauling to enormous SCAs is the main drawback to practice in reality [10, 11]. The advancement in massive MIMO technology can bridge the gap in wireless backhauling of SCAs and it is considered as a viable and cost-effective solution [12]. Small cell access points (SCAs) can localize the data traffic thereby minimizing the distance between the clients and transmitters resulting in less propagation loss and enhanced energy efficiency. Besides providing the enhancement in the SE and EE, massive MIMO and network densification are envisioned as prominent technologies of the 5G network and B5G [13]. With the recent trends such as massive MIMO and the network densification in B5G creates a natural concern to reduce the power consumption to attain thousand-fold energy efficiency [14]. Additionally, full-duplex (FD) communication paved its way with the recent developments in self interference cancellation capability via beamforming strategies and shared antenna methodology [15–19]. In Inband FD communication, the nodes are enabled to perform concurrent transmission and reception of information in the same frequency resources. Thus, FD communication attains remarkable enhancement in the SE of the system. Henceforth, the FD technology at the SCA and enabling massive MIMO at the macro base station (MBS) imparts an eminent architecture combining the benefits of aforesaid technologies.

1.1 Related work

The above-mentioned works highlight the effectiveness of massive MIMO systems, HetNet, and FD technology. Therefore, the work improvement achieved by utilizing the aforementioned technologies is discussed. The combination of Massive MIMO and small cell have grabbed significant research interest. In [20], distributed power allocation strategy in HetNet is analyzed and EE assuring a reduced transmission rate is validated. In [21], rate maximization and transmit power minimization subjected to power constraints are jointly addressed in HetNet. It is proved that the EE is improved. However, the above works focused on power optimization in HetNets with small cells but it did not consider the impact of massive MIMO technology on HetNet. In [22], spectral and energy efficiency is maximized by utilizing power allocation and antenna selection strategy in massive MIMO systems. In [23], a scalable power control strategy is analyzed in massive MIMO systems to maximize the SE and to provide maximum fairness among users in the network. In [24], Power optimization in massive MIMO systems with the zero-forcing (ZF) beamforming strategy is validated. The zero-forcing (ZF) beamforming strategy reduces the self interference thereby

enhancing the downlink (DL) rate. In [25], the power allocation method considering QoS constraints for massive MIMO systems and the impact of the number of clients and the antennas on EE is also discussed. The above-mentioned works concentrated on power optimization in massive MIMO systems and not on HetNet with small cells. In [26, 27], conceptualize massive MIMO based HetNet scenario is discussed. Here, the massive MIMO utilizes degrees of freedom and offers services to its clients at the same time and frequency band thus enhancing throughput of the system. Further in [28], the network power consumption is greatly enhanced by employing massive MIMO enabled HetNet with small cells. This analysis is done by considering dynamic and static power consumption. Here, MZF beamforming is utilized by the transmitters to serve the users. The downlink (DL) transmit power minimization subjected to QoS constraints at the users is achieved utilizing the MZF beamforming in [28]. In [29], the authors have discussed the eigen beamforming strategy for computing the channel capacity under specific power constraint considering all the antennas. The water filling algorithm is utilized to allocate power in various eigenmodes. It lacks accuracy due to the output restraint of the power amplifier. In [30], the analysis related to complexity has been analyzed and it is observed that the optimal system design can achieve energy and spectral efficiency with reduced complexity. Authors in [8, 19] examined the gain of massive MIMO and small cells together. Here, the power allocation and backhaul problem is not addressed. The FD technology remains as a backhaul solution in massive MIMO enabled HetNet with small cells as stated in [31, 32]. Authors in [18] have developed a self-backhaul strategy where SCAs are enabled with FD technology. As a consequence, SCAs permits the reception of information from the MBS while concurrently communicates the information to its clients in the DL. Similarly, SCAs permit the reception of information from its clients in the uplink (UL) while simultaneously communicates the information to the MBS. It has also manifested the efficacy of the FD self backhaul strategy without considering the interference issue in HetNet. Authors in [33, 34], discussed sum rate maximization and transmit power minimization guaranteeing QoS by incorporating power allocation strategies in FD enabled massive MIMO systems. Here, the backhaul transmit power is not considered in the power allocation strategy. The summary of the related works is presented in Table 1. From the literature, it is observed that extensive research is focused on power optimization in massive MIMO technology and HetNet with small cells individually. Very few of the research work focused on power optimization in massive MIMO enabled HetNet with small cells. Parameters such as sum rates, EE, SE, and fairness are maximized by utilizing a power allocation strategy in the network. Backhauling the massive MIMO enabled HetNet with small cells is an important research issue. Even though a massive

Table 1 Summary of the related works

Reference	Methodology	Parameter	System design	Beamforming Design is considered	Backhaul power allocation is considered
[20]	Power allocation	Maximize EE	HetNet with small cells	No	No
[21]	Power allocation	Rate maximization	HetNet with small cells	No	No
[22]	Power allocation And antenna selection	Maximize SE and EE	Massive MIMO	No	No
[23]	Power allocation	Maximize fairness & SE	Massive MIMO	No	No
[24]	Power optimisation	Rate maximisation	Massive MIMO	Yes	No
[25]	Power allocation	Improve EE	Massive MIMO	No	No
[28]	Power Optimisation	Improve EE	Massive MIMO enabled HetNet with small cells	Yes	No
[30]	Power optimisation	Improve EE	Massive MIMO enabled HetNet with small cells	Yes	No

MIMO enabled HetNet with small cells could furnish a high data rate between the clients and MBS, the transmissions occurring between the MBS and SCAs results as the bottleneck of the network. Therefore, a reliable backhaul solution is required to enhance the data rate of clients in the network. Thus, enabling FD technology at the SCA is considered as a backhaul solution. FD backhauling allows the transmission and reception of information using the same spectrum. However, power allocation becomes challenging when jointly considering massive MIMO enabled HetNet with FD small cells.

1.2 Contribution of the paper

We propose a HetNet architecture comprising of MBS enabled with massive MIMO overlaying multiple SCAs with FD capability serving macro user equipments (MUEs) and small cell user equipments (SUEs). Here, simultaneous transmissions occur from the MBS to its user (access link) and from the MBS to SCAs (backhaul link) at the same frequency band. The power allocation problem of the MBS and SCAs with FD capability is formulated as a non-convex optimization problem. Then it is reformulated as a convex problem utilizing semi-definite relaxation. Scaled beamforming design and power optimization algorithm is coherently addressed to maximize the system sum rate with reduced power consumption guaranteeing QoS at the clients. The complexity analysis has been performed to compute the optimal system performance.

1.3 Organization of the paper

The remaining sections of the article are organized as follows: Section 2 discusses the system model. Section 3 discusses the joint power optimization and scaled beamforming algorithm.

Section 4 illustrates the simulation result analysis and finally, the conclusion is discussed in section 5.

2 System model

The massive MIMO enabled HetNet with a small cell network comprising of one macro base station (MBS) equipped with a number of M antennas and randomly deployed N number of SCAs with a single antenna as depicted in Fig. 1. It is considered that the MBS is capable of providing information to K single-antenna MUEs and every SCA serves one single-antenna SUEs. Here K + N « M, which denotes massive MIMO is used and M can be a large value ranging from 8 to 100 or even more [28]. We assume that all the base stations and user terminals are synchronized and operated on TDD protocol. The variables or representation utilized for deriving the equations are presented as in Table 2.

2.1 Channel model

In channel modeling, the fading channel matrix is represented as $D = \left[d_{k,0} d_{k,0}^H, \ldots, d_{k,n} d_{k,n}^H \right]$. Rayleigh flat fading random variable is represented as $d_{k,0}^H \in C^{M \times 1}$ and $d_{k,n}^H \in C^{N \times 1}$

In addition, MBS employs MZF beamforming technique to perfectly eradicate the multiuser interference. The $x_{k,0}^m$ and $x_{k,n}^s$ denotes the data signals at the MBS and the nth SCA serving k user equipments (UE). It is obtained from the Gaussian codebook and it is represented as $x_{k,n}^s \sim CN(0, 1)$ for $n = 0, \ldots, N$. Then, n_k is a complex guassian noise variable and variance is σ_k^2. The beamforming vectors $z_{k,0}^m \in \mathbb{C}^{M \times 1}$, $z_{k,n}^s \in \mathbb{C}^{N \times 1}$ are multiplied with the data signals to acquire the transmitted signals.

Table 2 Variable/Representation used in the system model

Variable / Representation	Interpretation
M	Number of antennas in MBS
N	Number of SCAs
K	Number of MUEs and SUEs
P	Transmission power
d	Small scale fading
z	Precoding matrix
x	Data symbol
k	Index associated to k^{th} MUE
n	n^{th} SCA & its user index
$()^m$	Represents MBS
$()^s$	Represents SCAs
$()^b$	Represents backhaul

$$x_n = \sum_{k=1}^{K} z_{k,n}^s x_{k,n}^s, \qquad n = 0, \ldots., N \qquad (1)$$

Here $z_{k,n}^s \neq 0$, and this optimization variable is used to find the solution for 'n' transmitters that can provide services to the kth UE. The received signal at the kth MUE which experience the inter-tier interference from SCAs is written as

$$y_k^m = \sqrt{P_k^m} d_k^{m^H} z_k^m x_k^m + \sum_{n=1}^{N} \sqrt{P_n^s} d_{nk}^{s^H} x_n^s + n_k^m \qquad (2)$$

The first term in Eq. (2) represents the intended signal received by MUEs from the MBS and the subsequent term indicates the cross-tier interference from SCAs. The received signal-to-interference-plus-noise ratio (SINR) of kth MUE is derived using the Eq. (2) and it is as follows:

$$SINR_k^m = \frac{P_k^m \left\| d_k^{m^H} z_k^m \right\|^2}{\sum_{n=1}^{N} P_n^s d_{nk}^{s^{H}{}^2} + \sigma_k^2} \qquad (3)$$

SCAs acquire information from the MBS and concurrently transmit the information to SUEs utilizing the same frequency resource. Self-interference from itself and co-tier interference from other SCAs are the commonly occurring interference at the SCAs. Thus, the received signal at the nth SCA is written as

$$y_n^b = \sqrt{P_n^b}\, d_n^{b^H} z_n^b x_n^b + \sum_{n'=1,\neq n}^{N} \sqrt{P_{n'}^s}\, d_{n'n}^{s^H} x_{n'}^s + \sqrt{\gamma P_n^s}\, x_n^s$$
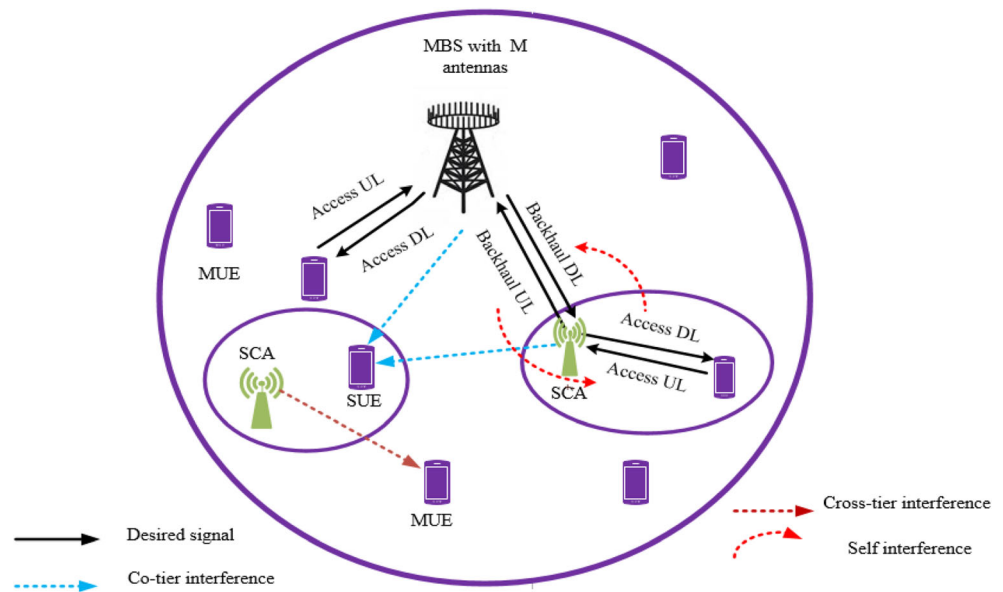$$+ n_n^b \qquad (4)$$

The first term in Eq. (4) represents the intended signal, the subsequent term indicates the co-tier interference and the third term indicates the self-interference and self-interference cancellation methods are utilized to evaluate the value of γ. The investigation carried out in this work is a common case. Hence, the received SINR at the nth SCA is represented as

$$SINR_n^b = \frac{P_n^b \left\| d_n^{b^H} z_n^b \right\|^2}{\sum_{n'=1,\neq n}^{N} P_{n'}^s d_{n'n}^{b^{H}{}^2} + \gamma P_n^s + \sigma_k^2} \qquad (5)$$

The SUEs suffer from co-tier interference due to MBS and cross-tier interference due to SCAs. Thus, the received signal at the nth SCA user can be written as

$$y_n^s = \sqrt{P_n^s} d_n^{s^H} x_n^s + \sum_{n'=1,\neq n}^{N} \sqrt{P_{n'}^s}\, d_{n'n}^{s^H} x_{n'}^s + \sum_{k=1}^{K} \sqrt{P_k^m}\, d_n^{m^H} z_k^m x_k^m,$$
$$+ \sum_{n'=1}^{N} \sqrt{P_{n'}^b} d_n^{m^H} z_n^b x_{n'}^b + n_n^s \qquad (6)$$

Fig. 1 Massive MIMO enabled HetNet with FD small cells

The first term in the above Eq. (6) denotes the intended signal, the subsequent term indicates the co-tier interference from SCAs, the third and fourth terms indicates the cross-tier interference from the MBS. Therefore, the received SINR at the nth SCA user is expressed as

$$SINR_n^s = \frac{P_n^s d_n^{s^{H^2}}}{\sum\limits_{k=1}^{K} P_k^m \left\| d_n^{m^H} z_k^m \right\|^2 + \sum\limits_{n'=1}^{N} P_{n'}^b \left\| d_n^{m^H} z_{n'}^b \right\|^2 + \sum_{n'=1, \neq n}^{N} P_{n'}^s d_{n'n}^{s^H} + \sigma_k^2} \quad (7)$$

3 Joint power optimization and scaled beamforming algorithm

In this section, problem realization is done and the beamforming algorithm with less complexity is discussed. The main objective is to attain power optimization while sustaining QoS. The QoS constraints denote the data rate [bits/s/Hz] that every UE must attain in parallel. It is denoted as $\log_2(1 + SINR_k) \geq \gamma_k$, where γ_k is known as the fixed QoS target. The aggregate SINR of the kth UE assuming the perfect channel estimation can be represented as

$$SINR_k = \frac{\left| d_{k,0}^H z_{k,0} \right|^2 + \sum_{n=1}^{N} \left| d_{k,n}^H z_{k,n} \right|^2}{\sum\limits_{i=1; i \neq k}^{K} \left(\left| d_{k,0}^H z_{i,0} \right|^2 + \sum_{n=1}^{N} \left| d_{k,n}^H z_{i,n} \right|^2 \right) + \sigma_k^2} \quad (8)$$

The total power consumed per subcarrier is denoted as $P_d + P_s$ where P_d, P_s are dynamic and static power [28].

$$P_d = \rho_o \sum_{k=1}^{K} \left\| z_{k,0} \right\|^2 + \sum_{n=1}^{N} \rho_n \sum_{k=1}^{K} \left\| z_{k,n} \right\|^2 \quad (9)$$

$$P_s = \frac{\eta_o}{C} M + \sum_{n=1}^{N} \frac{\eta_n}{C} N \quad (10)$$

Here, C denotes the number of subcarriers, ρ_o, ρ_n signifies the efficiency of power amplifiers at the MBS and SCA, while η_o, η_n denotes the circuit power per antenna at the MBS and SCA. Therefore, the power optimization while sustaining QoS is obtained by

$$\underset{z_{k,n} \forall k,n}{\text{minimize}} \, P_d + P_s \quad (11)$$

subject to $\log_2(1 + SINR_k) \geq \gamma_k \forall k$

$\sum_{k=1}^{K} z_{k,n}^H \, z_{k,n} \leq q_n \forall n$

The QoS constraints in the above-mentioned Eq. (11) make it a non-convex problem and it can be reformulated as a convex problem utilizing semi-definite relaxation. To achieve a convex semi-definite problem formulation from Eq. (11), the matrix is expected to be positive semi-definite and it is represented as $\mathbb{Z}_{k,n} = z_{k,n}^H z_{k,n} \forall n$ and the matrix rank is less than or

equal to 1 i.e., rank $(\mathbb{Z}_{k,n}) \leq 1$. Rank could be zero which implicates $\mathbb{Z}_{k,n} = 0$. Hence, by including MBS and SCAs, the expression is given as

$$\underset{z_{k,n} \geq 0 \forall k,n}{\text{minimize}} \sum_{n=0}^{N} \rho_n \sum_{k=1}^{K} \text{tr}(\mathbb{Z}_{k,n}) + P_s \quad (12)$$

subject to $\quad \text{rank}(\mathbb{Z}_{k,n}) \leq 1 \forall k, n$

$$\sum_{n=0}^{N} \left(d_{k,n}^H \right) \left(\left(1 + \frac{1}{\widetilde{\gamma}_k} \right) \mathbb{Z}_{k,n} - \sum_{k=1}^{K} \mathbb{Z}_{i,n} \right) d_{k,n} \geq \sigma_k^2 \forall k,$$

$\sum_{k=1}^{K} \text{tr}(\mathbb{Z}_{k,n}) \leq q_n \forall n$

Here, q_n and σ_k^2 denotes per-antenna constraints at the transmission node and variance. Then, the QoS target is transformed into SINR targets which are as follows.

The QoS target is given as $\log_2(1 + SINR_k) \geq \gamma_k \forall k$,

After applying antilog on both sides, we get $SINR_k \geq 2^{\gamma_k} - 1 \forall k$.

Substituting the $SINR_k$ value from Eq. (8) in the above-mentioned equation as

$$\frac{\left| d_{k,0}^H z_{k,0} \right|^2 + \sum_{n=1}^{N} \left| d_{k,n}^H z_{k,n} \right|^2}{\sum\limits_{i=1; i \neq k}^{K} \left(\left| d_{k,0}^H z_{i,0} \right|^2 + \sum_{n=1}^{N} \left| d_{k,n}^H z_{i,n} \right|^2 \right) + \sigma_k^2} \geq 2^{\gamma_k} - 1 \quad (13a)$$

The above equation can be rewritten considering MBS and SCAs

$$\frac{\sum_{n=0}^{N} \left| d_{k,n}^H z_{k,n} \right|^2}{\sum\limits_{i=1; i \neq k}^{K} \left(\left| d_{k,0}^H z_{i,0} \right|^2 + \sum_{n=1}^{N} \left| d_{k,n}^H z_{i,n} \right|^2 \right) + \sigma_k^2} \geq 2^{\gamma_k} - 1 \quad (13b)$$

$$\frac{\sum_{n=0}^{N} \left| d_{k,n}^H z_{k,n} \right|^2}{2^{\gamma_k} - 1} \geq \sum\limits_{i=1; i \neq k}^{K} \left(\left| d_{k,0}^H z_{i,0} \right|^2 + \sum_{n=1}^{N} \left| d_{k,n}^H z_{i,n} \right|^2 \right) + \sigma_k^2 \quad (13c)$$

$$\frac{\sum_{n=0}^{N} \left| d_{k,n}^H z_{k,n} \right|^2}{2^{\gamma_k} - 1} \geq \sum_{n=0}^{N} \left(\left| d_{k,n}^H z_{k,n} \right|^2 \right)$$

$$+ \sum_{i=1}^{K} \left(\sum_{n=0}^{N} \left| d_{k,n}^H z_{i,n} \right|^2 \right) + \sigma_k^2 \quad (13d)$$

$$\frac{\sum_{n=0}^{N} \left| d_{k,n}^H z_{k,n} \right|^2}{2^{\gamma_k} - 1} - \sum_{n=0}^{N} \left(\left| d_{k,n}^H z_{k,n} \right|^2 \right) - \sum_{i=1}^{K} \left(\sum_{n=0}^{N} \left| d_{k,n}^H z_{i,n} \right|^2 \right) \geq \sigma_k^2 \quad (13e)$$

$$\sum_{n=0}^{N} d_{k,n}^H \left(\left(1 + \frac{1}{2^{\gamma_k} - 1} \right) \mathbb{Z}_{k,n} - \sum_{i=1}^{K} \mathbb{Z}_{i,n} \right) d_{k,n} \geq \sigma_k^2 \quad (13f)$$

where QoS target is transformed to SINR target which is given by, $\widetilde{\gamma}_k = 2^{\gamma_k} - 1 \forall k$.

Equation (13a) to (13f) illustrate the procedure to convert non-convex optimization problem to convex optimization

problem (i.e) to convert Eqs. (11) to (12). Now, Eq. (12) indicates the convex problem excluding the rank constraints. Yet optimality could be attained by relaxing the constraints. As in [28], $\left\{ \mathbb{Z}_{k,n}^* \forall k, n \right\}$ is considered to be the optimal solution to Eq. (12) and every UE has three choices to attain optimality: $\mathbb{Z}_{k,n}^* = 0, 1 \leq n \leq N$; (when the MBS only serves the UE), $\mathbb{Z}_{k,0}^* = 0$ and $\mathbb{Z}_{k,n}^* = 0$ for i≠n (when the UE is served only by the nth SCA point), $\sum_{k=1}^{K} \text{tr}\left(\mathbb{Z}_{k,n}^* \right) = q_n$ (When the UE is served by a combination of MBS and SCAs). The convex optimization problem could provide an optimal solution in polynomial time using standard algorithms. To obtain optimal results, every UE is assigned only one transmitter even though UEs could be aided by multi-flow transmission. UEs which are very near to SCAs are merely served by it and the remaining UEs are served by the MBS. The transition areas surrounding SCA could not able to satisfy the QoS targets, so it leads to a change in the transition areas which has a multi-flow transmission. Thus, it minimizes transmission complexity.

3.1 Scaled beamforming approach

The optimal beamforming related to spatial soft-cell has moderate complexity but this becomes impracticable during the real time implementation with a large number of M and N. The centralized algorithm can be acquired utilizing primal or dual decomposition methods. It becomes non-viable to practice in reality since it requires iterative signaling of the parameters. Multi-flow ZF beamforming is less complex and non-iterative. When $n = 0 \dots N$ at the transmitter, the following equation is calculated.

$$u_{k,n} = \frac{\left(\sum_{i=1}^{K} \frac{1}{\sigma_i^2} d_{i,n} d_{i,n}^H + \frac{K}{\tilde{\gamma}_k q_n} I \right)^{-1} d_{k,n}}{\left\| \left(\sum_{i=1}^{K} \frac{1}{\sigma_i^2} d_{i,n} d_{i,n}^H + \frac{K}{\tilde{\gamma}_k q_n} I \right)^{-1} d_{k,n} \right\|} \forall k, \qquad (14)$$

Here the MBS resolves the convex optimization problem.

$$\begin{array}{c} \text{minimize} \\ P_{k,n} \geq 0 \forall k, n \end{array} \sum_{n=0}^{N} \rho_n \sum_{k=1}^{K} \left(P_{k,n} \right) + P_s$$

$$\text{subject to} \quad \sum_{k=1}^{K} P_{k,n} \leq q_{k,n} \forall n, \qquad (15)$$

$$\sum_{n=0}^{N} P_{k,n} \left(1 + \frac{1}{\tilde{\gamma}_k} \right) - \sum_{i=1}^{K} P_{k,n} \geq \sigma_k^2 \forall k$$

The allotment of power $(P_{k, n})^* \forall k$ provides a solution for Eq. (15) at the nth SCA and the calculation is as follows

$$z_{k,n} = \left(\sqrt{P_{k,n}} \right)^* u_{k,n} \forall k \qquad (16)$$

When ZF beamforming is applied in the above algorithm, the problem could be formulated as a power allocation issue which is represented in Eq. (15). It is less complex regardless of the massive antennas present in the base station. Since this algorithm does not work iteratively, only a few scalar parameters are varied among MBS and SCA to sustain the coordination. The UEs who are in the proximity of SCA are affected.

The conventional ZF technique nullifies the cross-tier interference of the users who are present in the cell edges. The system complexity is increased to nullify the cross-tier interference. Even though the cross-tier interference disappears, thermal noise is present. Therefore, it is limited and comparable in some aspects with that of thermal noise. Thus the complexity level is reduced by relaxing the interference constraints, and the number of antennas can be increased for providing a larger rate when compared to the ZF method.

A less complex optimal beamforming algorithm is achieved through scaling the noise by a factor of $\psi_{i, n}$ while sustaining the desired signal power. The non-iterative and less complex ZF beamforming serves as a source for the scaled beamforming algorithm. Here power optimization is accomplished with less complexity by scaling the interference noise power which is in the unit norm as in Eq. (17) and it is written as

$$\tilde{u}_{k,n} = \frac{\left(\sum_{i=1}^{K} \frac{1}{\sigma_i^2} d_{i,n} d_{i,n}^H + \left(\psi_{i,n} \right) \frac{K}{\tilde{\gamma}_k q_n} I \right)^{-1} d_{k,n}}{\left\| \left(\sum_{i=1}^{K} \frac{1}{\sigma_i^2} d_{i,n} d_{i,n}^H + \left(\psi_{i,n} \right) \frac{K}{\tilde{\gamma}_k q_n} I \right)^{-1} d_{k,n} \right\|} \forall k, \qquad (17)$$

W h e r e
$\psi_{i,n} = (M-1) + (i-n), \quad i = 1, \dots, K \text{ and } n = 1, \dots, N$

The allotment of power $(P_{k, n})^* \forall k$ provides a solution for Eq. (15) at the nth SCA and the calculation is as follows

$$z_{k,n} = \left(\sqrt{P_{k,n}} \right)^* \tilde{u}_{k,n} \forall k \qquad (18)$$

3.2 Power optimization algorithm

In massive MIMO enabled HetNet with FD small cell network interference between the network access and backhaul links is considered to be limiting factor which can hinder the system performance. Initially, beamforming is designed at the base stations to optimize the power consumption under QoS constraints. Then the power optimization is carried out through the power allocation algorithm. The power allocation (PA) algorithm is formulated for the access and backhaul part of the network to maximize the sum rates of users. Furthermore, we have considered the backhaul capacity to ensure the efficient allocation of power resources. The main aim is to

calculate the power required for transmission by MBS and SCAs assuring peak power constraints.

In the DL, SCAs permits the reception of information from the MBS while concurrently communicates the information to its clients at the same time and frequency band. Similarly, SCAs permit the reception of information from its clients in the UL while simultaneously communicates the information to the MBS. Here, in this study, SCAs are considered as special MUEs. In the DL, the MBS transmits information to MUEs and SCAs, and SCAs transfer the information to their clients concurrently in the same frequency band. In the UL, the SCAs receive information from their clients and transmit them to the MBS, and the MBS receives information from MUEs and SCAs simultaneously in the same frequency band. In massive MIMO enabled HetNet with FD small cells, the transmission or reception of the access and backhaul of SCAs is possible in the same frequency and time similar to the transmission or reception of information to the SUEs and MUEs. The main aim is to maximize the data rate of access part of the network while considering the backhaul capacity limits. The power optimisation problem is formulated as the maximization of the sum of user data rates.

Data Rate of MBS : $\qquad R_k^m = B\log_2\left(1 + SINR_k^m\right)$ (19)

Date Rate of Backhaul : $\qquad R_n^b = B\log_2\left(1 + SINR_n^b\right)$ (20)

Data rate of SCAs : $\qquad R_n^s = B\log_2\left(1 + SINR_n^s\right)$ (21)

The total data rate R is derived from SCAs, MUEs, SUEs represented by R_n^b, R_k^m, R_n^s is formulated as

$$R(P) = \sum_{k=1}^{K} R_k^m + \sum_{n=1}^{N} R_n^s + \sum_{n=1}^{N} R_n^b \qquad (22)$$

The power allocation strategy of the MBS and SCAs is written as $P = \left[P_1^m, \ldots., P_K^m, P_1^b, \ldots., P_N^b, P_1^s, \ldots., P_N^s\right]$. The Power allocation (PA) strategy adopted by the MBS and SCA to enhance the sum rate can be achieved by using

$$\begin{aligned}
&\max_{P} \; R(P) \\
\text{s.t.} \quad & S_1 : R_n^s \leq R_n^b, \forall n \\
& S_2 : \sum_{k=1}^{K} P_k^m \leq P_{max}^m \\
& S_3 : P_n^s \leq P_{max}^s, \forall n \\
& S_4 : P_n^b \leq P_{max}^b, \forall n \\
& S_5 : R_k^m \geq R_{min}, \forall k \\
& S_6 : R_n^s \geq R_{min}, \forall n
\end{aligned} \qquad (23)$$

Where S_1 denotes that the SCAs backhaul downlink rate should not be less than SCAs access downlink rate to assure QoS. Here, S_2, S_3 and S_4 specifies the transmit power constraint of the MBS, SCA, and backhaul link. The P_{max}^m and P_{max}^s represents the maximum transmit power of the MBS and the SCAs respectively. S_5 and S_6 denotes the minimum data rate requirement or QoS requisite of MUEs and SUEs.

The Eq. (23) denotes non-linear coupling among the optimization parameters. It is computationally intractable to find the optimal solution. So, a low complexity algorithm can be developed to compute the optimal solution. The coupled problem is solved by dividing it into small subproblems utilising eigenvalue decomposition method. In this power allocation algorithm, maximum transmit power is assigned in the MBS and the backhaul station i.e., SCA. The transmit power is reduced until the data rate difference becomes minimal. P_k is computed for all users in the network using the Eq. (24). The optimal power allocation according to the water filling algorithm is utilized to enhance the data rates in the access links by assuming the interference that occurs at backhaul as noise.

$$P_k = \begin{cases} \nu_k B - \dfrac{K}{A_k(N-K)}, & \text{if } A_k > \dfrac{1}{\nu_k} \\ 0 \; ; & \text{otherwise} \end{cases} \qquad (24)$$

Where B represents bandwidth, ν_k denotes the threshold for power allocation according to user priority. $\nu_k \in [0, 1]$ denotes each user's priority. In case of equal priority, $\nu_k = {}^1/_K$ for all k. This corresponds to water filling distribution with variable threshold levels that can be varied by the user priorities. Then, $A_k = \frac{\sigma_k^2 + P_k^b d_{nk}}{\gamma_k}$ is the kth MUEs link condition. Here σ_k^2 denotes the self-interference variance, P_k^b denotes the backhaul power, d_{nk} denotes the channel gain, and γ_k represents the interfering channel gain with respect to backhaul. The channel gains d_{nk} and γ_k follows a uniform distribution.

After determining the access power, both access and backhaul rates can be determined. If the backhaul rate R_k^b is greater than the access rate R_k^m, the backhaul power P_k^b is minimized by a factor of δ_{min}. If R_k^b is lesser than R_k^m, the MBS should minimize its transmission power P_k^m by a factor of δ_{min}. In this algorithm, the MBS and the SCA transmission powers are optimized along with the backhaul transmission power by considering backhaul capacity limits.

Power Allocation (PA) Algorithm:

Step 1:	Define the following parameters: a) Number of UE's: K b) The maximum transmitting power of MBS: P_{max}^m c) The maximum transmitting power of backhaul: P_{max}^b d) Minimum power δ_{min} e) Self-interference variance: σ_k^2
Step 2:	a) Set the initial counter value $c = 1$. b) Calculate the data rate difference $H_o = \left\| R_k^b - R_k^m \right\| > 0$ c) Set the backhaul power $P^b = P_{max}^b$ d) The total power used by MBS $P^m = P_{max}^m$
Step 3:	Calculate P_k, where $k = 1, 2 \ldots \ldots \ldots K$ using equation (24)
Step 4:	a) Calculate $R_{m,c} = \sum_{k=1}^{K} R_k^m$ b) Calculate $R_{b,c} = \sum_{k=1}^{K} R_k^b$
Step 5:	Calculate the difference between Step 4(a) and Step 4(b) (i.e) $H_c = \left\| R_{b,c} - R_{m,c} \right\|$
Step 6:	If $H_{c-1} \leq H_c$ then Stop the counter c

Step 7:	If $R_k^{b,c} > R_k^{m,c}$ then
	
	    Reduce backhaul power (i.e) $P^b = P^b - \delta_{min}$
	
	    Increment the counter value c by one.
	
	else
	
	    Reduce the total power of MBS (i.e) $P^m = P^m - \delta_{min}$
	
	    Increment the counter value c by one

Step 8:	Return to Step 3 for further iteration.

4 Simulation results and analysis

This section evaluates the performance of the joint power optimization and scaled beamforming algorithm in the massive MIMO enabled HetNet with FD small cell networks. The convex optimization problem has been efficiently carried out utilizing algorithmic toolbox SeDuMi which is accessible in the modeling language CVX [35]. Table 3 list the parameters utilized for simulation.

The total power consumption versus QoS target per user is illustrated in Fig. 2 with M = 50 and N = 2. The PA and scaled Beamforming scheme are compared with PA and ZF Beamforming, MZF beamforming, and MBS schemes. It is observed that total power per subcarrier of PA and scaled

Table 3 Simulation parameters

Parameters	Values
The radius of the cell	500 m
Number of MBS antenna	100
Number of SCA	2
Number of users	10
Bandwidth	10 MHz
MBS transmit power (max)	46 dBm
SCAs transmit power (max)	20 dBm
Number of channel realizations	10
Least distance between the MBS and its user	35 m
Carrier frequency	2 GHz
Number of Subcarriers	600
Subcarrier Bandwidth	30 kHz
Penetration loss	20 dB
Noise Figure	5 dB
Power amplifier efficiency	$\rho_o = = 2.577$, $\rho_n = 19.23 \; \forall \; n$
Circuit power per antenna	$\eta_o = 189mW$, $\eta_n = 5.6mW \; \forall \; n$
Per antenna constraints	$q_0 = 66$, $q_n = 0.08mW \; \forall \; n$
δ_{min}	0.05 W
Noise power spectral density	−174 dBm/Hz
QoS constraint per user	2 bits/s/Hz

beamforming scheme, PA and ZF beamforming scheme, MZF beamforming, and MBS scheme increases with an increase in QoS target per user.

Table 4 shows comparisons of total power consumption and QoS target per user between MBS, MZF

beamforming, PA, and ZF beamforming and PA and scaled beamforming. From Table 4, it observed that total power per subcarrier is reduced marginally in PA and ZF beamforming when compared to the MZF beamforming technique. This is due to the suitable power allocation method is employed in the network. Further, the total power per subcarrier is reduced in PA and scaled beamforming method when compared to MZF beamforming, because appropriate joint power allocation scheme with scaled beamforming method is implemented in the network. So, PA and scaled beamforming method outperformed when compared to MZF beamforming, PA and ZF beamforming and MBS schemes.

Figures 3 and 4 shows the DL sum rate and UL sum-rate against σ^2 in dB. DL and UL sum rate is assessed for FD mode without PA and beamforming, MZF beamforming, FD with PA and ZF beamforming, FD with PA, and scaled beamforming. When the value σ^2 is large, the sum rates obtained during UL and DL transmissions are decreased. It is because the larger the value of σ^2, it indicates the significant interference resulting in the increased backhaul power consumption. Therefore, the available power for MUEs is low and on the other hand, MBS assigns a smaller amount of power to SCAs backhaul link which can affect the achievable sum rate of MUEs and SUEs during the DL and UL transmissions.

Tables 5 and 6 show the comparisons of the DL sum rate and UL sum-rate respectively. From Tables 5 and 6, it is noticed that the sum-rate is marginally increased in FD with PA and ZF beamforming when compared to MZF beamforming. This is due to the appropriate power
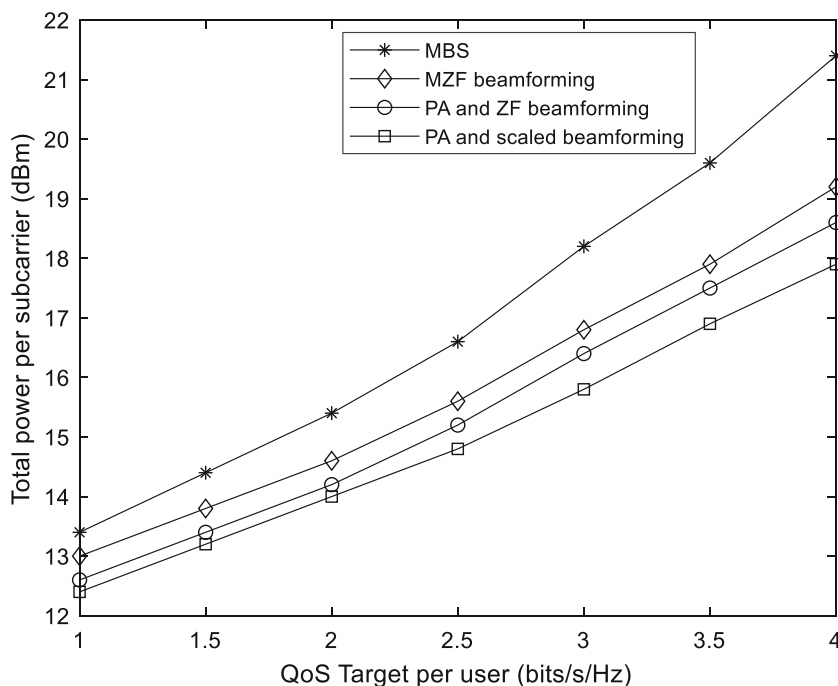
Fig. 2 Total power consumption versus QoS constraints

342

Peer-to-Peer Netw. Appl. (2021) 14:333–348

Table 4 Comparison of Total power consumption and QoS target per user

QoS Target per users	Total power per subcarrier (dBm)				% of Total power per subcarrier reduced	
	MBS	MZF beamforming	PA and ZF beamforming	PA and scaled beamforming	MZF beamforming (vs PA and ZF beamforming)	MZF beamforming (vs PA and scaled beamforming)
1	13.5	13	12.5	12.2	3.84%	6.15%
1.5	14.5	13.5	13	12.8	3.84%	5.18%
2	15.5	14.5	13.7	13.5	5.51%	6.89%
2.5	16.5	15	14.5	14.3	3.33%	4.66%
3	18.0	16	15.5	15	3.12%	6.25%
3.5	19.6	17.2	16.5	15.5	4.06%	9.88%
4	21.5	18.5	17.7	17.2	4.32%	7.02%

allocation method is employed in the network. Further, the sum rate is increased in FD with PA and scaled beamforming when compared to MZF beamforming. Conclusively, the FD with PA and scaled beamforming outperforms when compared with other approaches because the PA algorithm assigns the power to the MUEs, SUEs and the scaled beamforming algorithm reduces the interference that occurs during transmissions.

4.1 Complexity analysis

The complexity analysis has been carried out by varying the number of transmission antennas at the MBS, SCAs, and the number of UEs. Figure 5 clearly shows the total power consumption of the network based on the different number of UEs. It is inferred that when the UEs in the network increases,

eventually it increases the power consumption. Figure 6 shows the total power consumption of the network based on the different number of antennas at the MBS. If the number of transmission antennas at the MBS increases, it creates additional complexity resulting in increased power consumption. Tables 7 and 8 illustrate the comparison of total power per subcarrier and the number of UEs, and total power per subcarrier and the number of MBS respectively. It is evident from Tables 7 and 8, is that the FD with PA with scaled beamforming algorithm provides better results when compared to other approaches. Complexity analysis carried out relying on the different number of UEs is computed utilizing the relation

$$\text{Complexity} = \text{Number of UEs} \log_{10}\left(P_{\text{Average}}\right) \quad (25)$$

$$\text{Complexity} = \text{Antennas at the MBS} \log_{10}\left(P_{\text{Average}}\right) \quad (26)$$

Fig. 3 Downlink (DL) sum rate
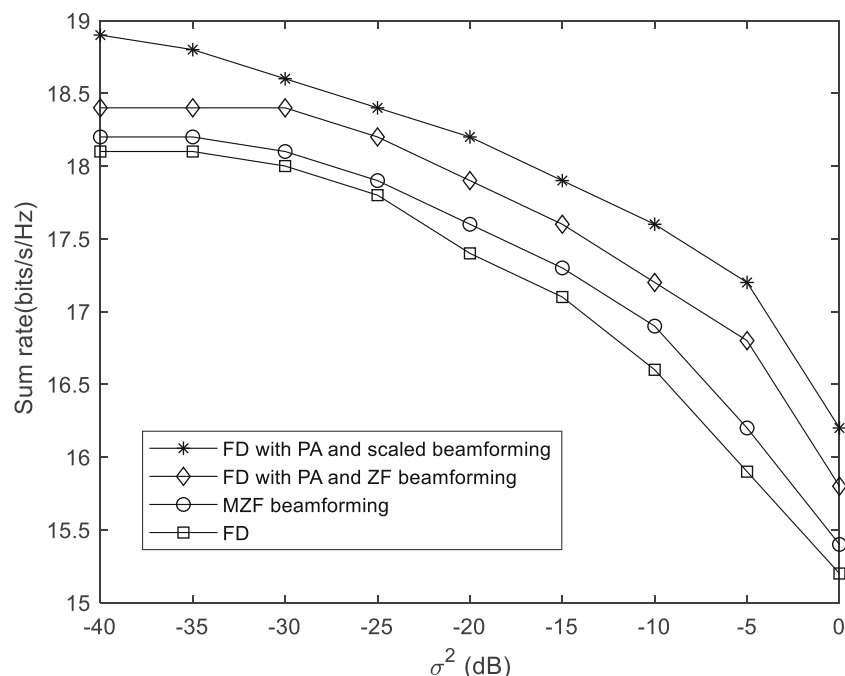
Fig. 4 Uplink (UL) sum rate
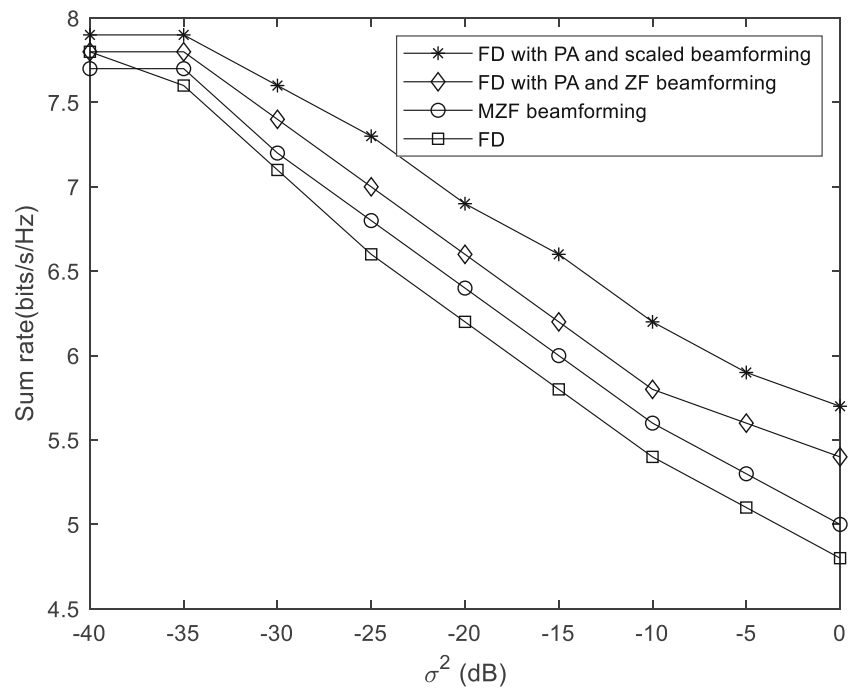
Table 5 Comparison of Downlink sum rate

σ^2 dB	Sum rate (bits/s /Hz)				% of improvement in Sum rate	
	FD	MZF beamforming	FD with PA and ZF beamforming	FD with PA and scaled beamforming	MZF beamforming (vs) FD with PA and ZF beamforming	MZF beamforming (vs) FD with PA and scaled beamforming
- 40	18.1	18.2	18.4	18.9	1. 09%	3.84%
- 35	18.1	18.2	18.4	18.8	1. 09%	3.30%
−30	18.0	18.1	18.4	18.6	1. 65%	2. 76%
−25	17.8	17.9	18.2	18.4	1. 67%	2. 79%
−20	17.4	17.6	17.9	18.2	2. 27%	3. 40%
−15	17.1	17.2	17.6	17.9	2. 33%	4. 06%
−10	16.6	16.9	17.2	17.6	2. 38%	4. 14%
−5	15.8	16.2	16.8	17.2	3. 70%	6. 17%
0	15.2	15.3	15.8	16.3	3. 26%	6.53%

Table 6 Comparison of Uplink sum rate

σ^2 dB	Sum rate (bits/s /Hz)				% of improvement in Sum rate	
	FD	MZF beamforming	FD with PA and ZF beamforming	FD with PA and scaled beamforming	MZF beamforming (vs) FD with PA and ZF beamforming	MZF beamforming (vs) FD with PA and scaled beamforming
- 40	7.8	7.7	7.8	7.9	1. 29%	2. 59%
- 35	7.6	7.7	7.8	7.9	1. 29%	2. 59%
−30	7.1	7.2	7.4	7.6	2. 77%	5. 55%
−25	6.6	6.8	7.1	7.3	4. 41%	7. 35%
−20	6.2	6.4	6.7	6.9	4. 68%	7. 81%
−15	5.8	6.0	6.3	6.6	5 .0%	10 .0%
−10	5.4	5.6	5.9	6.3	5. 34%	12. 50%
−5	5.1	5.3	5.6	6.0	5. 66%	13. 27%
0	4.8	5.0	5.4	5.7	8 .0%	14. 00%

Table 7 Comparison of Total power per subcarrier and Number of UEs

Number of UEs	Total power per subcarrier (dBm)				% of Total power per subcarrier reduced	
	FD	MZF beamforming	FD with PA and ZF beamforming	FD with PA and scaled beamforming	MZF beamforming (vs FD with PA and ZF beamforming	MZF beamforming (vs) FD with PA and scaled beamforming
6	15.44	14.6	13.80	13.0	5. 47%	10. 95%
8	16.42	14.8	14.0	13.4	5. 40%	9. 45%
10	17.26	15.4	14.8	13.8	3. 89%	10. 38%
12	18.34	16.2	15.5	14.2	4. 32%	12. 34%
14	19.26	17.4	16.6	15.3	4. 59%	12. 06%
16	20.96	18.7	17.9	16.6	4. 27%	11. 22%
18	22.3	20.8	19.7	18.5	5. 22%	11.05%
20	23.67	22.8	22.4	21.2	1. 75%	7. 01%

Table 8 Comparison of Total power per subcarrier and antennas at MBS

Antenna at the MBS	Total power per subcarrier (dBm)				% of Total power per subcarrier reduced	
	FD	MZF beamforming	FD with PA and ZF beamforming	FD with PA and scaled beamforming	MZF beamforming (vs FD with PA and ZF beamforming	MZF beamforming (vs) FD with PA and scaled beamforming
20	25.7	19.0	18.0	16.2	5. 26%	14. 73%
30	19.2	17.0	16.3	15.6	4. 11%	8. 23%
40	18.5	16.5	16.2	15.9	1. 81%	3 .63%
50	17.2	15.3	14.7	14.4	3. 92%	5. 88%
60	16.8	15.1	14.3	14.1	5. 29%	6. 66%
70	16.7	15.3	14.8	14.7	3. 26%	3. 92%
80	16.3	15.4	15.0	15.0	2. 59%	2. 59%
90	16.2	15.5	14.9	14.8	3. 8 7%	4. 51%
100	16.0	14.8	14.6	14.5	1. 35%	2. 02%

Fig. 5 Total power per subcarrier versus Number of UEs with M = 50, N = 2
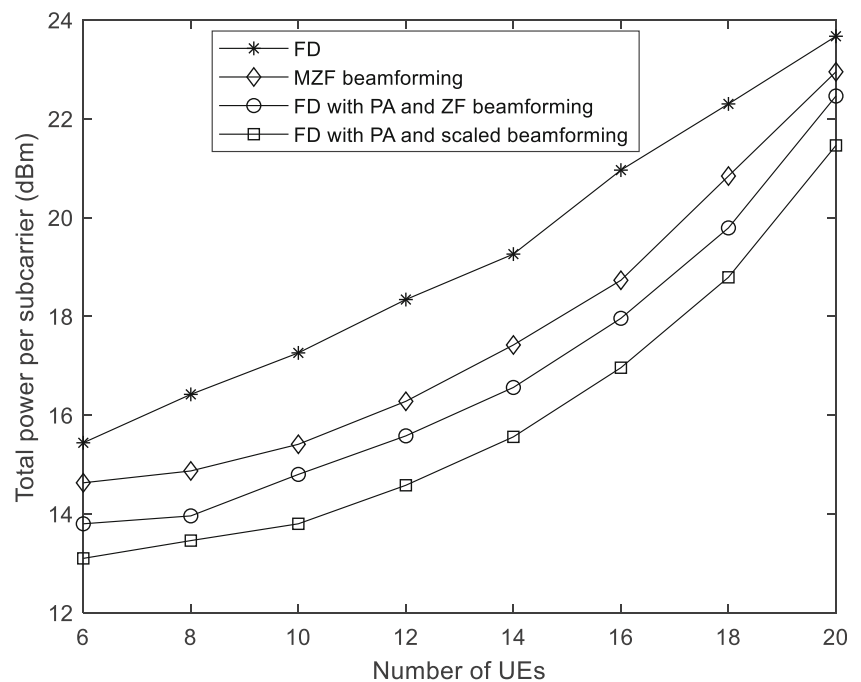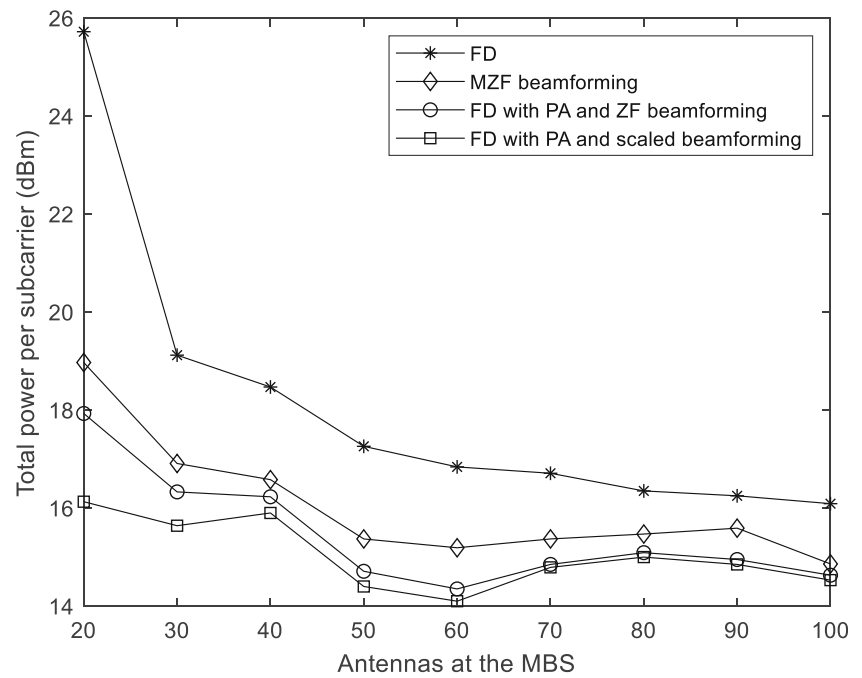
Fig. 6 Total power per subcarrier versus Antennas at the MBS

Where ($P_{Average}$) denotes the average of the total power consumed while differing the number of transmission antennas at the MBS and UEs.

From Figs. 7 and 8, it is observed that the system becomes more complicated with the inclusion of the total number of UEs and the number of antennas at the MBS with the increased total power consumption. Thus, it can be concluded that the complexity possesses a direct relation with the increment in the different numbers of UEs and antennas at the MBS, which have a great impact on the average total power consumption. Shannon channel capacity theorem is directly proportional to the bandwidth. The Eqs. (25) and (26) are assessed with the existing Shannon channel capacity theorem. Thus, the

Fig. 7 Complexity analysis on differing the number of UEs when M = 50, N = 2
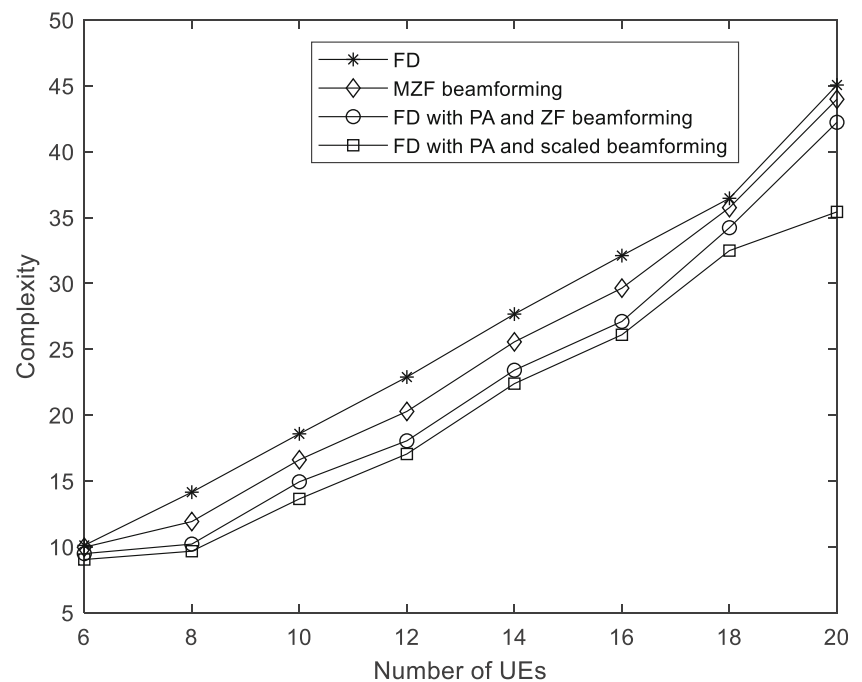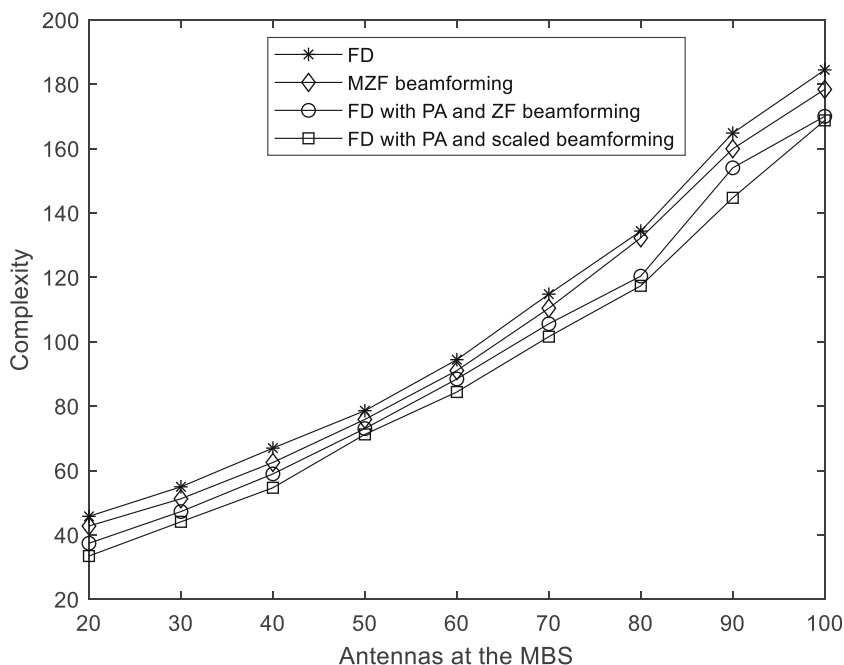
Fig. 8 Complexity analysis on differing the number of antennas

FD with PA and scaled beamforming algorithm optimizes the power with reduced complexity and provides better performance when compared to FD with PA and ZF beamforming, MZF beamforming, and FD methods.

4.2 Computational complexity analysis

The number of additions and multiplications required to compute the total power per subcarrier, downlink, and uplink sum-rate of the proposed algorithm is illustrated in Table 9. The number of SCA's are represented as N and number of user's are represented as K.

5 Conclusion

This paper has evaluated the performance of the joint power optimization and scaled beamforming algorithm in a massive MIMO enabled HetNet with small cells. The FD transmission mode enables to utilize the access and backhaul links concurrently in the same frequency band. Moreover, we express the power allocation problem as an optimization problem considering co-tier and cross tier interference. Utilizing the concepts of convex optimization, tractable, and computable analytical modeling is done to enhance the sum rates and minimize the power consumption while operating in FD mode. Furthermore,

Table 9 Computational complexity of the proposed algorithm

Transmit power per subcarrier		
Description	Number of additions	Number of Multiplications
PA and ZF beamforming	$4N^2(1+K^2)+NK(8N+1)+6N+2(K+1)$	$4N^2(K+1)^2+4N(3K+5)+K+7$
PA and scaled beamforming	$4N^2(1+K^2)+NK(8N+1)+6N+2(K+1)$	$4N^2(K+1)^2+2N(6K+11)+K+11$
Downlink Sum-rate		
Description	Number of additions	Number of Multiplications
FD with PA and ZF beamforming	$4N^2(1+K^2)+NK(8N+1)+6N+3K+2$	$4N^2(K+1)^2+4N(3K+5)+2K+7$
FD with PA and scaled beamforming	$4N^2(1+K^2)+NK(8N+1)+6N+3K+2$	$4N^2(K+1)^2+2N(6K+11)+2K+11$
Uplink Sum-rate		
Description	Number of additions	Number of Multiplications
FD with PA and ZF beanforming	$4N^2(1+K^2)+NK(8N+1)+7N+K+2$	$4N^2(K+1)^2+3N(4K+7)+K+7$
FD with PA and scaled beamforming	$4N^2(1+K^2)+NK(8N+1)+7N+K+2$	$4N^2(K+1)^2+K(12N+1)+23N+1$

along with the power optimization, the scaled beamforming technique is used to sustain the low complexity and it is compared with the conventional ZF beamforming and the optimal beamforming technique considering only MBS. The PA algorithm assigns the power to the MUEs and SUEs to enhance the sum rates and the scaled beamforming technique reduces the interference issue. From the numerical results, it is evident that the joint power optimization and scaled beamforming technique escalates the network capacity and outperforms the PA along with conventional ZF beamforming and the optimal case without considering PA and beamforming technique. Conclusively, the complexity analysis has been done and the results clearly show that optimizing the number of transmission antennas as well as users remains a crucial design parameter to obtain the optimal system performance.

References

1. Cisco VNI (2018) Cisco visual networking index: forecast and trends, 2017–2022. White Paper 1
2. Nguyen LD, Tuan HD, Duong TQ, Dobre OA, Poor HV (2018) Downlink beamforming for energy-efficient heterogeneous networks with massive MIMO and small cells. IEEE Trans Wirel Commun 17(5):3386–3400
3. Lu L, Li GY, Swindlehurst AL, Ashikhmin A, Zhang R (2014) An overview of massive MIMO: benefits and challenges. IEEE J Select Topics Signal Process 8(5):742–758
4. Björnson E, Larsson EG, Marzetta TL (2016) Massive MIMO: ten myths and one critical question. IEEE Commun Mag 54(2):114–123
5. Zhang J, Björnson E, Matthaiou M, Ng DWK, Yang H, Love DJ (2020) Prospective multiple antenna technologies for beyond 5G. arXiv preprint arXiv:1910.00092 v3
6. Van Chien T, Canh TN, Björnson E, Larsson EG (2020) Power control in cellular massive MIMO with varying user activity: a deep learning solution. IEEE Trans Wirel Commun:1. https://doi.org/10.1109/TWC.2020.2996368
7. Zeydan E, Dedeoglu O, Turk Y (2020) Experimental evaluations of TDD-based massive MIMO deployment for Mobile network operators. IEEE Access 8:33202–33214
8. Hoydis J, Ten Brink S, Debbah M (2013) Massive MIMO in the UL/DL of cellular networks: how many antennas do we need? IEEE J Select Areas Commun 31(2):160–171
9. Sheikhi A, Razavizadeh SM, Lee I (2020) A comparison of TDD and FDD massive MIMO systems against smart jamming. IEEE Access 8:72068–72077
10. Li B, Zhu D, Liang P (2015) Small cell in-band wireless backhaul in massive MIMO systems: a cooperation of next-generation techniques. IEEE Trans Wirel Commun 14(12):7057–7069
11. Tabassum H, Sakr AH, Hossain E (2016) Analysis of massive MIMO-enabled downlink wireless backhauling for full-duplex small cells. IEEE Trans Commun 64(6):2354–2369
12. Ragunathan S, Perumal D (2020) Enhancement of energy efficiency in massive MIMO network using superimposed pilots. J Ambient Intell Humanized Comput:1–8
13. Chen X, Ng DWK, Yu W, Larsson EG, Al-Dhahir N, Schober R (2020) Massive access for 5G and beyond. arXiv preprint arXiv:2002.03491
14. Matthaiou M, Yurduseven O, Ngo HQ, Morales-Jimenez D, Cotton SL, Fusco VF (2020) The road to 6G: ten physical layer challenges for communications engineers. arXiv preprint arXiv:2004.07130
15. Xie Y, Li B, Zuo X, Yan Z, Yang M (2018) Performance analysis for 5G beamforming heterogeneous networks. Wirel Netw:1–15
16. Hoydis J, Hosseini K, Ten Brink S, Debbah M (2013) Making smart use of excess antennas: massive MIMO, small cells, and TDD. Bell Labs Technical J 18(2):5–21
17. Pitaval RA, Tirkkonen O, Wichman R, Pajukoski K, Lahetkangas E, Tiirola E (2015) Full-duplex self-backhauling for small-cell 5G networks. IEEE Wirel Commun 22(5):83–89
18. Lagunas E, Lei L, Maleki S, Chatzinotas S, Ottersten B (2017) Power allocation for in-band full-duplex self-backhauling. In 2017 40th International Conference on Telecommunications and Signal Processing (TSP). IEEE, pp 136–142
19. Chen L, Yu FR, Ji H, Leung VC, Li X, Rong B (2016). A full-duplex self-backhaul scheme for small cell networks with massive MIMO. In 2016 IEEE International Conference on Communications (ICC). IEEE, pp 1-6
20. Mao T, Feng G, Liang L, Qin S, Wu B (2015) Distributed energy-efficient power control for macro–femto networks. IEEE Trans Veh Technol 65(2):718–731
21. Mili MR, Hamdi KA, Marvasti F, Bennis M (2015) Joint optimization for optimal power allocation in OFDMA femtocell networks. IEEE Commun Lett 20(1):133–136
22. Gao H, Su Y, Zhang S, Diao M (2019) Antenna selection and power allocation design for 5G massive MIMO uplink networks. China Commun 16(4):1–15
23. Ghazanfari A, Cheng HV, Björnson E, Larsson EG (2020) Enhanced fairness and scalability of power control schemes in multi-cell massive MIMO. IEEE Trans Commun 68(5):2878–2890
24. Tripathi SC, Trivedi A, Rajoria S (2018) Power optimization of cell free massive MIMO with zero-forcing beamforming technique. In 2018 Conference on Information and Communication Technology (CICT). IEEE, pp 1-4
25. Zhang J, Jiang Y, Li P, Zheng F, You X (2016) Energy efficient power allocation in massive MIMO systems based on standard interference function. In 2016 IEEE 83rd Vehicular Technology Conference (VTC Spring). IEEE, pp 1-6
26. Duarte M, Sabharwal A, Aggarwal V, Jana R, Ramakrishnan KK, Rice CW, Shankaranarayanan NK (2013) Design and characterization of a full-duplex multiantenna system for WiFi networks. IEEE Trans Veh Technol 63(3):1160–1177
27. Björnson E, Sanguinetti L, Hoydis J, Debbah M (2015) Optimal design of energy-efficient multi-user MIMO systems: is massive MIMO the answer? IEEE Trans Wirel Commun 14(6):3059–3075
28. Björnson E, Kountouris M, Debbah M (2013) Massive MIMO and small cells: improving energy efficiency by optimal soft-cell coordination. In ICT 2013. IEEE, pp 1-5
29. Telatar E (1999) Capacity of multi-antenna Gaussian channels. Eur Trans Telecommun 10(6):585–595
30. Sofi IB, Gupta A, Jha RK (2019) Power and energy optimization with reduced complexity in different deployment scenarios of massive MIMO network. Int J Commun Syst 32(6):e3907
31. Kela P, Costa M, Turkka J, Leppanen K, Jantti R (2016) Flexible backhauling with massive mimo for ultra-dense networks. IEEE Access 4:9625–9634
32. Li B, Zhu D, Liang P (2015) Small cell in-band wireless backhaul in massive MIMO systems: a cooperation of next-generation techniques. IEEE Trans Wirel Commun 14(12):7057–7069
33. Korpi D, Riihonen T, Valkama M (2016) Self-backhauling full-duplex access node with massive antenna arrays: power allocation

348

Peer-to-Peer Netw. Appl. (2021) 14:333–348

and achievable sum-rate. In 2016 24th European Signal Processing Conference (EUSIPCO). IEEE pp 1618-1622

34. Korpi D, Riihonen T, Valkama M (2017) Inband full-duplex radio access system with self-backhauling: transmit power minimization under QoS requirements. In 2017 IEEE International Conference on Acoustics, Speech and Signal Processing (ICASSP). IEEE, pp 6558-6562

35. CVX Research Inc. (2012) CVX: Matlab software for disciplined convex programming, version 2.0 beta. http://cvxr.com/cvx

Publisher's note Springer Nature remains neutral with regard to jurisdictional claims in published maps and institutional affiliations.

Malini Balachandran received her B.Tech. degree in Electronics and Communication Engineering from B.S.Abdur Rahman University in 2015 and M.Tech. degree in Communication Engineering from Vellore Institute of Technology, Vellore in 2017. She is currently pursuing PhD degree in Vellore Institute of Technology, Vellore. Her research interests include Wireless communication and Signal processing. Email id: malinichandar@gmail.com

Noor Mohammed Vali Mohamad received his B.E., Degree in Electronics and Communication Engineering from Madras University, Tamil Nadu, India, in 1999 and the M.E., Degree in Communication Systems from Madurai Kamarj University, Tamil Nadu, India in 2003. He received his Ph. D in Wireless Communication and Networking from Vellore Institute of Technology, Vellore, Tamil Nadu, India. Currently he is Associate Professor in School of Electronics Engineering, VIT, Vellore, Tamil Nadu India. He is a member in IEEE and life member in ISTE. He has published more than fifty papers in reputed journals and conferences. His research interests include Wireless Communication, Advanced Wireless Networks, Massive MIMO and Green Communication. Email ID: noorb4u@gmail.com